IEEE Access
Multidisciplinary ⋮ Rapid Review ⋮ Open Access Journal

Received March 3, 2022, accepted April 20, 2022, date of publication April 25, 2022, date of current version May 19, 2022.

Digital Object Identifier 10.1109/ACCESS.2022.3170432

Research on Emergency Collision Avoidance System of Man-Machine Cooperative Driving Vehicles Based on Additional Yaw Moment Control

CHAOCHUN YUAN[1], SONGLIN LV[1], JIE SHEN[2], LONG CHEN[1], YOUGUO HE[1], AND SHUOFENG WENG[1]

[1]Automotive Engineering Research Institute, Jiangsu University, Zhenjiang 212013, China
[2]Department of Computer and Information Science, University of Michigan–Dearborn, Dearborn, MI 48128, USA

Corresponding author: Chaochun Yuan (yuancc_78@163.com)

This work was supported in part by the National Natural Science Foundation of China under Grant 51775247 and Grant 52172346.

ABSTRACT Drivers of man-machine cooperative driving intelligent vehicles are affected by driving skills, physiological reactions, and other factors. Under emergency conditions, they often subconsciously forcefully take over control rights and produce unreasonable stress steering, which brings new accident risks to vehicles. To avoid collisions, this paper proposes an emergency collision avoidance control strategy for man-machine cooperative driving vehicles. In the collision avoidance path planning layer, considering the obstacle distance, road adhesion coefficient, vehicle speed, steering wheel stress angle, and driver's linear steering cognition, a circular arc lane-change path is designed. The curvature mutation is smoothed using the third-order Bezier function. In the tracking control layer, a method of additional yaw moment control is designed by using the model predictive control (MPC) algorithm to track the path. The accuracy and safety of vehicle tracking are guaranteed only by adjusting the braking torque of each wheel of the vehicle, to correct the unreasonable input when the driver forces to take over. The co-simulation results show that the collision avoidance control system can effectively correct the unreasonable input during forced take-over, and ensure the safety of stress steering.

INDEX TERMS Man-machine cooperative driving vehicles, additional yaw moment control, emergency collision avoidance system, model predictive control.

I. INTRODUCTION

The vehicle emergency collision avoidance system is one of the necessary active safety functions of intelligent vehicles. It requires intelligent vehicles to perceive their state and the surrounding environment, predict sudden traffic accidents in the path planning process and adopt methods to reduce the possibility of accidents, and optimize the target value of the control system so that it can effectively correct the unreasonable input when the driver forces to take over.

At present, most researches focus on the collision avoidance control of autonomous vehicles without considering the driver-in-the-loop, and tracking the planned path by controlling the wheel angle [1]–[4]. For man-machine cooperative driving intelligent vehicles, more researches on handover between autonomous driving and human driving. Russell *et al.* studied the handover of vehicles between full autonomous driving and full human driving [5], and the study indicated that designing for autonomous driving should carefully consider the period of compromised vehicle steering behavior during the handover of control. Othersen *et al.* considered the interaction between driver's cognitive take-over ability [6], the situational complexity, and various dimensions of a Non-driving Related (NDR) task to improve the driver's ability to have take-over control after a period of automated driving. Sentouh *et al.* presented a new cooperative control method [7], which manages the control authority between the autonomous driving system and the

The associate editor coordinating the review of this manuscript and approving it for publication was Hiram Ponce.

driver based on driver monitoring and the risk assessment. However, there are few studies on the driver forced to take over the vehicle for steering control under emergency conditions, and if the collision avoidance system still takes the front wheel turning angle as the control variable or directly to the control of the autonomous driving system under this condition, it will seriously affect the driver's trust in the collision avoidance system. Therefore, the man-machine cooperative control of emergency collision avoidance system considering the driver-in-the-loop needs further research.

The vehicle emergency collision avoidance system usually includes collision avoidance path planning and trajectory tracking control. The commonly used collision avoidance lane-changing paths include paths generated based on the sine function [8], seventh-order Bezier curve [9], and fifth-degree polynomial [10], [11], etc. Path calculation based on the sine function is simple and smooth, but the maximum value of path curvature appears at the starting point and the ending point, which makes the vehicle unable to meet the constraint conditions. The path generated based on the seventh-order Bezier curve can meet the constraint conditions of collision avoidance, but it needs to determine too many target points and the calculation is large, which limits the real-time performance. The path generated based on the fifth-degree polynomial has the advantage of continuous curvature without mutation, but the path does not meet the driver's cognition of steering and is not suitable for man-machine cooperative driving vehicles.

In recent years, the tracking control algorithms that have been studied more include proportion integral derivative (PID) control [12], optimal preview control [13], and model predictive control (MPC) algorithm based on vehicle kinematics or dynamics model [14]–[16]. The PID control algorithm tracks the desired path according to the vehicle's driving position deviation. The algorithm is simple, but the acceleration mutation will affect the trajectory tracking effect, which is not suitable for emergency collision avoidance conditions. The optimal preview control algorithm aims to minimize the tracking deviation in the preview window, and the control quantity is mostly the front wheel angle of the vehicle, so that the vehicle can accurately track the desired path, which is not suitable for the driver's forced steering. The model predictive control algorithm can constrain the intermediate state variables of vehicles, and determine the importance of each parameter in the tracking control process with different weight coefficients, which is suitable for solving multi-constrained problems.

For the emergency collision avoidance system of man-machine cooperative driving vehicles, this paper adopts different circular arc lane-changing paths based on the distance to obstacles, road adhesion coefficient, vehicle speed, steering wheel stress angle, and driver's linear steering cognition, and uses the third-order Bezier function to smooth at the curvature mutation, and establishes a lateral safety distance model to determine whether there is a risk of collision. The model predictive control algorithm is designed according to the changes of state variables and constraints during the vehicle stress emergency steering, and the additional yaw moment to ensure the tracking accuracy and safety is calculated and distributed proportionally to the vertical load, and the unreasonable input during the forced take-over is effectively corrected by controlling the braking torque of each wheel. Finally, a co-simulation environment was built using Matlab/Simulink-CarSim to verify the effectiveness and superiority of the system.

The main contributions of this paper include:

1. The improved circular arc lane-changing path conforms to the current environmental constraints, the vehicle dynamic characteristics, and the driver's steering cognition, so that the ordinary driver can know the path for collision avoidance in advance and make the corresponding operation in time.

2. The designed model predictive control algorithm conforms to the constraints of vehicle state variables, and the calculated additional yaw moment is reasonably distributed to ensure the accuracy and safety of vehicle tracking. The unreasonable input during forced takeover is effectively corrected by controlling the braking torque of each wheel, which reduces the risk of sudden traffic accidents of man-machine cooperative driving intelligent vehicles.

This paper is organized as follows. In Section II, the vehicle dynamics model is given. In Section III, the emergency steering driver model with adaptive preview distance is established. In Section IV, the emergency steering path is designed and analyzed. In Section V, the model predictive control algorithm is designed. In Section VI, the simulation results are analyzed. Finally, some concluding remarks of this paper are presented in Section VIII.

II. VEHICLE DYNAMICS MODEL

Under the premise of ensuring the stability and safety of vehicle trajectory tracking, to improve the accuracy of vehicle trajectory tracking and reduce the calculation amount in the control process, and to meet the real-time performance of the system, this paper uses the three degrees of freedom (3DOF) vehicle dynamics model [17]. Meanwhile, the necessary simplification and assumptions are made as follows:

1) Assuming that the intelligent vehicle is driving on a horizontal road, without considering vertical motion.
2) Assuming that the vehicle is a rigid body, ignoring the influence of the suspension system.
3) Assuming that the left and right angles of the vehicle are consistent, without considering the influence of the Ackermann angle.
4) Vehicle roll and pitch motion are not considered.
5) The influence of air resistance is not considered.

According to the above assumptions, the intelligent vehicle is simplified into the three degrees of freedom vehicle dynamics model with longitudinal, lateral, and yaw. Let the origin of the oxy coordinate system coincide with the vehicle's center of mass, and OXY is the global coordinate system, as shown in Fig. 1.

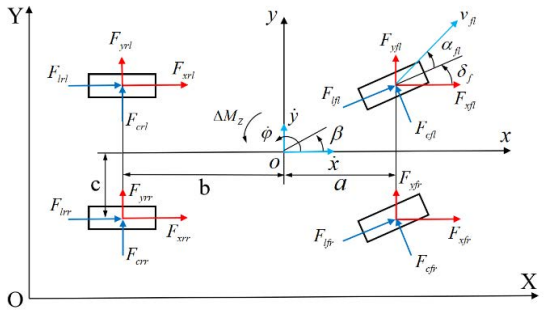

FIGURE 1. Vehicle dynamics model.

The vehicle dynamics can be described as:

$$\begin{aligned} m\ddot{x} &= m\dot{y}\dot{\varphi} + F_{xfl} + F_{xfr} + F_{xrl} + F_{xrr} \\ m\ddot{y} &= -m\dot{x}\dot{\varphi} + F_{yfl} + F_{yfr} + F_{yrl} + F_{yrr} \\ I_z\ddot{\varphi} &= a\left(F_{yfl} + F_{yfr}\right) - b\left(F_{yrl} + F_{yrr}\right) \\ &\quad + c\left(-F_{xfl} + F_{xfr} - F_{xrl} + F_{xrr}\right) + \Delta M_z \end{aligned} \tag{1}$$

where m is the total vehicle mass, $\dot{x}$ and $\dot{y}$ are the longitudinal and lateral velocity respectively, $\ddot{x}$ and $\ddot{y}$ are the longitudinal and lateral acceleration respectively, F_{xij} and F_{yij} are the longitudinal and lateral tire forces of the ijth wheel, ij denotes fl, fr, rl, and rr, which refers to front left, front right, rear left, and rear right wheel respectively, I_z is the vehicle moment of inertia about the z-axis, $\ddot{\varphi}$ is the vehicle yaw acceleration, a is the distance of the front-axle to the mass center, b is the distance of the rear-axle to the mass center, c is the half of the distance between wheels, ΔM_z is the additional yaw moment.

The coordinate conversion of the vehicle body coordinate system oxy to the global coordinate system OXY is described as:

$$\begin{aligned} \dot{X} &= \dot{x}\cos\varphi - \dot{y}\sin\varphi \\ \dot{Y} &= \dot{x}\sin\varphi + \dot{y}\cos\varphi \end{aligned} \tag{2}$$

In this paper, considering only the front wheel steering, the longitudinal and lateral forces generated by the four wheels in the x-axis and y-axis directions of the vehicle body coordinate system are described as:

$$\begin{aligned} F_{xfl} &= F_{lfl}\cos\delta_f - F_{cfl}\sin\delta_f \\ F_{yfl} &= F_{lfl}\sin\delta_f + F_{cfl}\cos\delta_f \\ F_{xfr} &= F_{lfr}\cos\delta_f - F_{cfr}\sin\delta_f \\ F_{yfr} &= F_{lfr}\sin\delta_f + F_{cfr}\cos\delta_f \\ F_{xrl} &= F_{lrl} \\ F_{yrl} &= F_{crl} \\ F_{xrr} &= F_{lrr} \\ F_{yrr} &= F_{crr} \end{aligned} \tag{3}$$

where F_{lij} and F_{cij} are the longitudinal and lateral forces of the ijth wheel in the wheel coordinate system, δ_f is the front wheel steering angle.

Referring to the Magic Formula tire model, the longitudinal force and lateral forces of the tire are described as:

$$\begin{aligned} F_l &= f_l\left(\alpha, s, \mu, F_z\right) \\ F_c &= f_c\left(\alpha, s, \mu, F_z\right) \end{aligned} \tag{4}$$

Combining Equations (1) to (4), the steering dynamics of the intelligent vehicle can be analyzed to obtain the vehicle nonlinear dynamics model, the vehicle system state space equation can be rewritten as:

$$\dot{\xi} = f\left(\xi, u\right) \tag{5}$$

III. EMERGENCY STEERING DRIVER MODEL

To better study the driver-in-the-loop vehicle emergency collision avoidance system and obtain the steering wheel angle change during emergency collision avoidance, it is necessary to establish an emergency steering driver model. In the general steering manipulation process, the visual preview information of the driver comes from far and near two regions. The preview near point information makes the driver reduce the lateral displacement deviation, and the preview far point information makes the driver predict the curvature of the road ahead in advance [18]–[20]. However, in the case of emergency collision avoidance, the driver cannot predict the distance information in advance in a very short time. Therefore, the single-point preview driver model can better reflect the driver's stress steering mechanism.

According to the preview following theory, the lateral error that the driver always wants to reach the preview point after driving is zero, as shown in Fig. 2. The lateral position at the preview point is described as:

$$y\left(t + \Delta t\right) = y\left(t\right) + \Delta t \cdot \dot{y}\left(t\right) + \frac{\Delta t^2}{2}\ddot{y}\left(t\right) \tag{6}$$

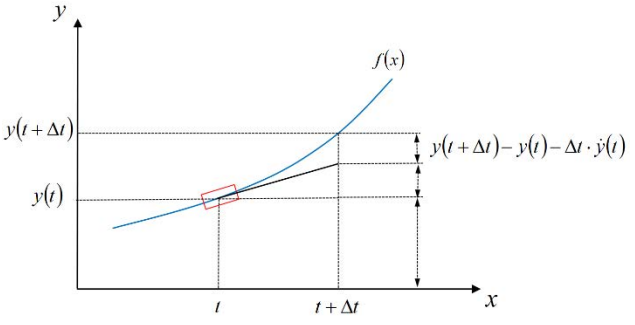

FIGURE 2. Single-point preview driver model.

The preview distance d is described as:

$$d = v \cdot \Delta t \tag{7}$$

And considering the vehicle kinematics.

$$\begin{aligned} \ddot{y}\left(t\right) &= v^2/R \\ \delta_f &= L/R \end{aligned} \tag{8}$$

The relationship between steering wheel angle and front wheel steering angle is described as:

$$\delta_{sw} = i \cdot \delta_f \tag{9}$$

Combining Equations (6) to (9), the steering wheel angle is described as:

$$\delta_{sw} = \frac{2iL}{d^2} \left(y\left(t + \Delta t\right) - y\left(t\right) - \Delta t \cdot \dot{y}\left(t\right) \right) \tag{10}$$

Therefore, only selecting the appropriate preview distance can conform to the real driver steering behavior. The real driver's preview distance isn't fixed in emergency collision avoidance, that is, the preview line should be adjusted adaptively with the curvature of the target path and the vehicle speed. When the vehicle speed is high and the curvature of the target path is small, the driver's preview distance should be increased adaptively. When the vehicle speed is low and the curvature of the target path is large, the driver's preview distance should be reduced adaptively.

Based on the above analysis, this paper proposes an emergency steering driver model with adaptive preview distance, that is, when the driver is in emergency steering, the preview distance is adaptively adjusted with vehicle speed and the curvature of the target path. Although the preview styles of different drivers are different, the change trend of preview distance of each driver is consistent. Different empirical coefficients are used to simulate, and the preview distance is described as:

$$d = \min\left(d_0 + \frac{k_1 \cdot V}{e^{k_2 \cdot \rho}}, D_{MF} \right) \tag{11}$$

where d_0 is the initial preview distance, reference scholars Land and Horwood research, set the initial preview distance of 6 meters, k_1 and k_2 are the empirical coefficients of speed and path curvature for different drivers respectively. D_{MF} is the longitudinal distance between the vehicle and the obstacle.

The emergency steering driver model with adaptive preview distance established in this section has a clear physical meaning, and can well conduct steering control, which largely reflects the emergency steering behavior of real drivers.

IV. EMERGENCY STEERING PATH PLANNING

A. COLLISION AVOIDANCE MULTI-CONSTRAINT DESIGN

The driving environment around the vehicle is complex and changeable. To ensure that the man-machine cooperative driving vehicle can avoid collisions in the process of emergency steering [21], it is necessary to design the emergency collision avoidance process with multi-constraints based on the characteristics of the driving environment and dynamics. The aim is comprehensive to reflect the rationality of vehicle emergency steering path and the safety of emergency collision avoidance.

To study the emergency situation, the vehicle can no longer avoid collision only by braking, but needs to take steering lane-change to avoid collision. This paper first clarifies the driving environment before collision avoidance, as shown in Fig. 3.

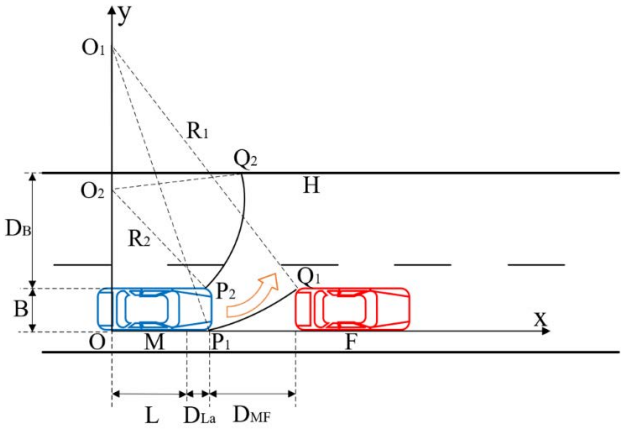

FIGURE 3. Emergency steering spatial constraints. M is the host vehicle, F is the obstacle vehicle in front, H is the road guardrail.

1) SPATIAL CONSTRAINT

The principle of spatial constraints is that the driver, in the face of unexpected emergencies, will produce steering lane-change collision avoidance needs. In this process, the most dangerous is to collide with the obstacle vehicle F in this lane, so the lower boundary of the spatial constraint is obtained by making a circular arc from the starting point of the host vehicle M to the critical point of the collision to the obstacle vehicle F. Taking the minimum turning radius of the host vehicle M as another arc, and limited by the road guardrail H, the upper boundary of the spatial constraint is obtained. The scope of emergency steering space constraints as shown in Fig. 3.

Assuming that the host vehicle and the obstacle vehicle are both of the same model, the coordinate system is established as shown in Fig. 3. And the O point coordinate is (x_M, y_M), the O_1 point coordinate is (x_M, y_1), the O_2 point coordinate is (x_M, y_2), the P_1 point coordinate is $(x_M + L + D_{La}, y_M)$, the P_2 point coordinate is $(x_M + L + D_{La}, y_M + B)$, the Q_1 point coordinate is $(x_M + L + D_{La} + D_{MF}, y_M + B)$, the Q_2 point coordinate is $\left(x_{Q2}, y_M + B + D_B\right)$. Where B is the vehicle width, D_B is the distance from the left side of the host vehicle to the road guardrail, L is the vehicle wheelbase, D_{La} is the vehicle front overhang, D_{MF} is the longitudinal distance between the host vehicle M and the obstacle vehicle F.

The circular arc $P_1\_Q_1$ satisfies the relationship of Equation (12):

$$(x - x_M)^2 + (y - y_1)^2 = R_1^2 \tag{12}$$

where $R_1^2 = (y_1 - B - y_M)^2 + (L + D_{La} + D_{MF})^2$. The equation of the circular arc $P_1\_Q_1$ can be obtained by substituting the coordinates of the points P_1 and Q_1 into Equation (12) respectively.

The circular arc $P_2\_Q_2$ satisfies the relationship of Equation (13):

$$(x - x_M)^2 + (y - y_2)^2 = R_2^2 \tag{13}$$

where $R_2 = R_{\min} - B$, $R_{\min}$ is the minimum turning radius of the host vehicle M. The equation of the circular arc $P_2\_Q_2$ can be obtained by substituting the coordinates of the points P_2 and Q_2 into Equation (13) respectively.

2) STABILITY CONSTRAINTS

The principle of stability constraints is that the yaw rate and the sideslip angle of mass center will increase rapidly when the driver is steering rapidly. When the upper limit of the two aspects is exceeded, the stability of the vehicle will deteriorate [22]. The upper limit of yaw rate and sideslip angle are directly related to road adhesion coefficient. The upper limit of yaw rate is $\omega_{\max} = 0.85\mu g/v_x$ [23], and the upper limit of side-slip angle is $\beta_{\max} = \arctan(0.02\mu g)$. Among them, the yaw rate ω represents the vehicle steering characteristics, which is more reflected in the stability. The sideslip angle of mass center β represents the deviation from the reference trajectory in the vehicle steering process, which is more reflected in the vehicle trajectory tracking [24].

When the vehicle is braked by the left and right side wheels, the additional yaw moment will be produced, can be described as:

$$\begin{aligned} \Delta M_z &= I_z \cdot \Delta\omega \\ \omega &= \frac{v}{R} \end{aligned} \tag{14}$$

The above equation shows that when the wheel braking force is the maximum value, the resulting limit additional yaw moment will increase or decrease the yaw rate of the vehicle. At a certain speed, the radius of the steering trajectory R is inversely proportional to the yaw rate ω, and there exists a minimum value of the radius of the steering trajectory.

B. EMERGENCY STEERING PATH ANALYSIS

The ordinary driver's cognition of vehicle steering in the face of an emergency is often based on linearity [25]. The reason is that people will actively decelerate when driving a vehicle steering in daily life, resulting in the driving experience accumulated by ordinary drivers mostly in low-speed conditions, which is suitable for vehicle linear model. To avoid collisions, the driver's steering intention is an ideal circular arc steering trajectory, but this steering trajectory has a sudden change in curvature at the junction of the two arcs, which is to be avoided in the steering process. Therefore, in this paper, the smoothing process at the junction of circular arcs is considered in trajectory generation.

The Bezier curve is a curve that can limit the curve range through the control points, and the curvature of the third-order Bezier curve is continuous. Using this curve in the design of vehicle steering path can reduce the requirements of curvature mutation on steering control, reduce the difficulty of control and improve the control effect. The third-order Bezier curve equation is described as:

$$\begin{aligned} B(t) &= P_0(1-t)^3 + 3P_1 t(1-t)^2 + 3P_2 t^2(1-t) + P_3 t^3, \\ & t \in [0, 1] \end{aligned} \tag{15}$$

where P_0, P_1, P_2, and P_3 are control points of the Bezier curve.

For higher safety requirements, spatial constraints and stability constraints are considered in emergency steering path generation. From the spatial constraint and stability constraint in the previous section, the value range of the emergency steering radius R at the vehicle's center of mass is described as:

$$R_2 + \frac{B}{2} \le R \le R_1 - \frac{B}{2} \& R \ge \frac{v_x^2}{0.85\mu g} \tag{16}$$

Considering that the impact on the vehicle should be minimized under the premise of ensuring safety, different emergency steering radius R are set for different driver stress reactions, as shown in Table 1.

TABLE 1. The value of emergency steering radius R.

Driver stress steering radius R'	Emergency steering radius R
$R' \le \max\left\{R_2 + \frac{B}{2}, \frac{v_x^2}{0.85\mu g}\right\} + \frac{\Delta R}{3}$	$R = \max\left\{R_2 + \frac{B}{2}, \frac{v_x^2}{0.85\mu g}\right\} + \frac{\Delta R}{3}$
$\max\left\{R_2 + \frac{B}{2}, \frac{v_x^2}{0.85\mu g}\right\} + \frac{\Delta R}{3} \le R' \le R_1 - \frac{B}{2} - \frac{\Delta R}{3}$	$R = R_1 - \frac{B}{2} - \frac{\Delta R}{2}$
$R_1 - \frac{B}{2} - \frac{\Delta R}{3} \le R'$	$R = R_1 - \frac{B}{2} - \frac{\Delta R}{3}$

Where ΔR is the difference of the range of values, that is, $\Delta R = (R_1 - B/2) - \max\left\{R_2 + B/2, v_x^2/0.85\mu g\right\}$, different emergency steering radius R corresponding to different circular arc emergency steering path and its curvature change.

To verify the smoothing effect of the third-order Bezier curve on the intersection of circular trajectories, the vehicle and road environment parameters were selected as shown in Table 2. The curvature change before processing is shown in Fig. 4.

TABLE 2. Vehicle parameters and road environment parameters.

Symbol	Parameters	Values
L	Wheelbase	2.603m
D_{La}	Front overhang	0.82m
B	Vehicle width	1.706m
$R_{\min}$	Minimum turning radius	5.5m
D_{MF}	Distance from the obstacle vehicle	20m
V_1	Velocity of the host vehicle	20m/s
V_2	Velocity of the obstacle vehicle	0m/s
W	Lane width	3.75m
μ	Road adhesion coefficient	0.85

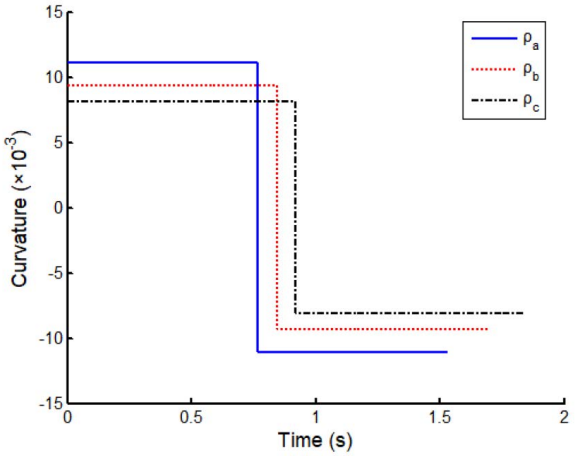

FIGURE 4. Before processing: Curvature change of circular arc emergency steering path.

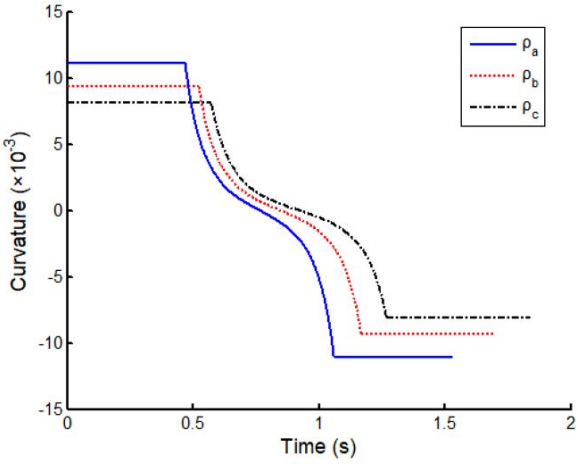

FIGURE 5. After processing: Curvature change after smoothing at circular arc junction.

The curvature change after smoothing the circular arc junction with third-order Bezier curve is shown in Fig. 5.

Fig. 4 and Fig. 5 describe the time response of the curvature change. After the third-order Bezier curve processing, the curvature change at the circular arc junction is improved, and the steering path becomes more reasonable.

C. LATERAL SAFETY DISTANCE MODEL

There are few existing lateral safety distance models. For man-machine cooperative driving intelligent vehicles in the process of emergency obstacle avoidance steering, to avoid collision accidents with obstacles or guardrails, a multi-factor lateral limit safety distance model under this condition is established for research.

The steering radius R_m of the vehicle at high speed steering is analyzed. The steering motion is shown in Fig. 6, ignoring the Ackermann angle when steering, and assuming that the

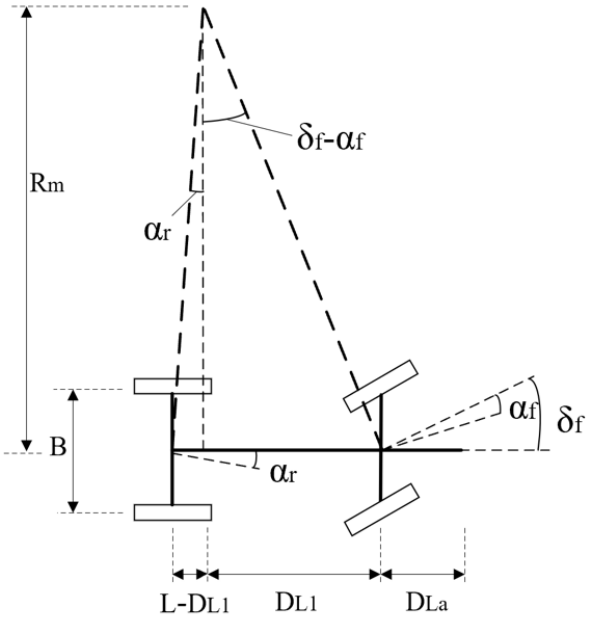

FIGURE 6. Steering motion of the vehicle.

steering angle of the inside and out-side front wheels is consistent.

According to the geometric relationship, it can be calculated that the vehicle steering radius R_m is described as:

$$D_{L1} = \frac{L \cdot \tan\left(\delta_f - \alpha_f\right)}{\tan\left(\alpha_r\right) + \tan\left(\delta_f - \alpha_f\right)} \tag{17}$$

$$R_m = \frac{D_{L1}}{\tan\left(\delta_f - \alpha_f\right)} = \frac{L}{\tan\left(\alpha_r\right) + \tan\left(\delta_f - \alpha_f\right)} \tag{18}$$

where D_{L1} is the distance from point of steering radius perpendicular to wheelbase to forward shaft, α_f and α_r are sideslip angle of front and rear wheels.

When the vehicle is driving on the road, in the process of emergency collision avoidance steering when encountering an unexpected situation, it has the risk of corner collision with the obstacle vehicle in front and the road guardrail. The relative position relationship between the host vehicle and the obstacle vehicle, and between the host vehicle and the road guardrail are shown in Fig. 7.

By defining $D_{L1a} = D_{L1} + D_{La}$, the establishment of a lateral safety distance model between the host vehicle and the obstacle vehicle:

$$D_{y-obc} = \sqrt{\left(D_{L1a} + D_{MF} + V_2 t_1\right)^2} - \sqrt{\left(R_m + \frac{B}{2}\right)^2 + D_{L1a}^2} \tag{19}$$

$$t_1 = \frac{\xi - \varepsilon}{w_o} \tag{20}$$

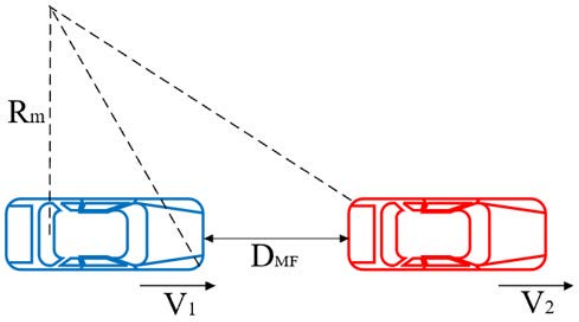

(a) Start steering between the host vehicle and the obstacle vehicle

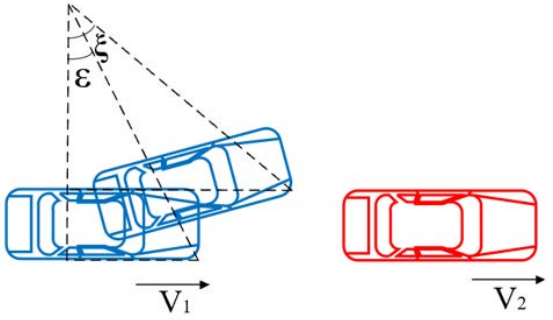

(b) During steering between the host vehicle and the obstacle vehicle

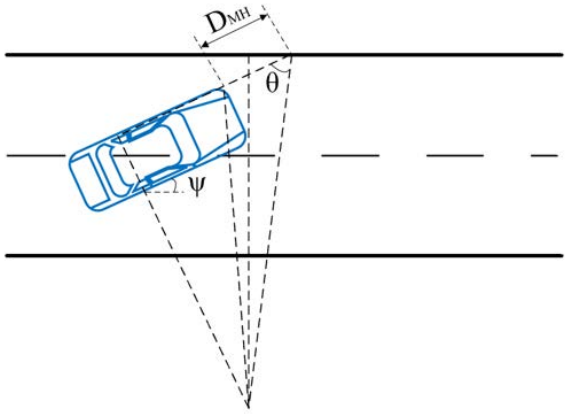

(c) Start steering between the host vehicle and the road guardrail

FIGURE 7. The relative position relationship.

$$\varepsilon = \arctan\left(\frac{D_{L1a}}{R_m + \frac{B}{2}}\right) \tag{21}$$

$$\xi = \arccos\left(\frac{R_m - \frac{B}{2}}{\sqrt{D_{L1a}^2 + \left(R_m + \frac{B}{2}\right)^2}}\right) \tag{22}$$

$$w_o = \frac{V_1}{\sqrt{D_{L1a}^2 + \left(R_m + \frac{B}{2}\right)^2}} \tag{23}$$

where V_1 is the velocity of the host vehicle, V_2 is the velocity of the obstacle vehicle, t_1 is the critical time of vehicle avoiding corner collision.

Establishment of lateral safety distance model between the host vehicle and the road guardrail:

$$D_{y-gua} = \sqrt{(D_{L1a} + D_{MH})^2 + \left(R_m + \frac{B}{2}\right)^2} \cdot \sin(\psi + \theta) - \sqrt{\left(R_m + \frac{B}{2}\right)^2 + D_{L1a}^2} \tag{24}$$

$$\psi = \int_0^{t_2} \omega dt \tag{25}$$

$$\theta = \arctan\left(\frac{R_m + \frac{B}{2}}{D_{L1a} + D_{MF}}\right) \tag{26}$$

where D_{MH} is the distance between the host vehicle and the road guardrail, ψ is the vehicle yaw angle, t_2 is the time for the driver to start reverse steering.

In Equations (19) and (24), D_{MF} and D_{MH} are obtained from the actual measurement by millimeter wave radar, V_2 is calculated from the distance D_{MF} and the velocity V_1.

V. EMERGENCY COLLISION AVOIDANCE TRAJECTORY TRACKING CONTROL

In the aspect of trajectory tracking control, model predictive control (MPC) does not require high accuracy of the whole vehicle model compared with other control algorithms [26], [27], and can effectively deal with multivariate problems and constrains the vehicle intermediate state to improve the trajectory tracking ability and ensure the robustness and stability of the system. In this section, the emergency collision avoidance trajectory tracking controller is designed based on the MPC algorithm.

A. PREDICTIVE MODEL

Considering Equation (5), the nonlinear dynamic model of intelligent vehicle is described as:

$$\dot{\xi}_{dyn} = f_{dyn}\left(\xi_{dyn}, u_{dyn}\right) \tag{27}$$

In this model, the state variables are defined as $\xi_{dyn} = [\dot{x}, \dot{y}, \varphi, \dot{\varphi}, X, Y]^T$ and the control variable is $u_{dyn} = \Delta M_z$.

To simplify the operation, the model needs to be linearized, according to the state trajectory obtained from the input constant control variable and the deviation of the actual state variables of the system, the linear time-varying equation is described as, Equations (28)–(30), shown at the bottom of the next page.

where $\frac{\partial f_{\dot{x}}}{\partial \dot{x}} = -\frac{2C_{cf}\delta_f(\dot{y}+a\dot{\varphi})}{m\dot{x}^2}$,
$\frac{\partial f_{\dot{y}}}{\partial \dot{x}} = -\dot{\varphi} + \frac{2C_{cf}(\dot{y}+a\dot{\varphi})+2C_{cr}(\dot{y}-b\dot{\varphi})}{m\dot{x}^2}$,
$\frac{\partial f_{\dot{\varphi}}}{\partial \dot{x}} = \frac{2[aC_{cf}(\dot{y}+a\dot{\varphi})-bC_{cr}(\dot{y}-b\dot{\varphi})]}{I_z\dot{x}^2}$.

The Equation (28) is discretized by the forward Euler method, and the discrete state space expression is described as:

$$\xi_{dyn}(k+1) = A_{dyn}(k)\,\xi_{dyn}(k) + B_{dyn}(k)\,u_{dyn}(t) \tag{31}$$

where $A_{dyn}(k) = I + TA_{dyn}(t)$, $B_{dyn}(k) = TB_{dyn}(t)$.

B. CONSTRAINT CONDITION

To meet the requirements of stability and safety [28], it is necessary to limit the dynamic characteristics and lateral displacement of the intelligent vehicle in the process of emergency collision avoidance steering at high speed.

Referring to the relevant literature [23], [29], the yaw rate constraint is $-0.85\mu g/v_x \le \omega \le 0.85\mu g/v_x$. Steering to avoid collision on the road with standard width of 3.75m cannot collide with the guardrail on both sides of the road, so the lateral displacement constraint is $B/2 - 1.875 \le Y \le 5.625 - B/2$. Considering the limit constraint of the control variable in the control process, the additional yaw moment constraint is $-F_z\mu B/4 \le \Delta M_z \le F_z\mu B/4$.

C. OPTIMIZATION SOLUTION

To improve the trajectory tracking accuracy and stability of the intelligent vehicle in the process of emergency collision avoidance steering, the objective function of trajectory error, control increment, and relaxation factor is established [30], [31].

$$\begin{aligned} &J\left(\xi_{dyn}(t), u_{dyn}(t-1), \Delta U_{dyn}(t)\right) \\ &= \sum_{i=1}^{N_P} \left\| \eta_{dyn}(t+i|t) - \eta_{dyn,ref}(t+i|t) \right\|_Q^2 \\ &\quad + \sum_{i=1}^{N_C-1} \left\| \Delta u_{dyn}(t+i|t) \right\|_R^2 + \rho\varepsilon^2 \end{aligned} \tag{32}$$

where N_P is the prediction horizon, N_C is the control horizon, Q and R are the weight matrix, ε is the relaxation factor, ρ is the weight matrix of relaxation factor.

Considering the constraints, the optimization problem of trajectory tracking controller can be described as:

$$\begin{aligned} \min_{\Delta U_{dyn},\varepsilon} \quad & \sum_{i=1}^{N_P} \left\| \eta_{dyn}(t+i|t) - \eta_{dyn,ref}(t+i|t) \right\|_Q^2 \\ & + \sum_{i=1}^{N_C-1} \left\| \Delta u_{dyn}(t+i|t) \right\|_R^2 + \rho\varepsilon^2 \\ s.t.\ & \Delta U_{dyn,\min} \le \Delta U_{dyn,t} \le \Delta U_{dyn,\max} \\ & U_{dyn,\min} \le A\Delta U_{dyn,t} + U_{dyn,t} \le U_{dyn,\max} \\ & y_{hc,\min} \le y_{hc} \le y_{hc,\max} \\ & y_{sc,\min} - \varepsilon \le y_{sc} \le y_{sc,\max} + \varepsilon \\ & \varepsilon > 0 \end{aligned} \tag{33}$$

where $\Delta U_{dyn,t}$ is the increment of the control variable at time t, y_{hc} is the hard constraint output, y_{sc} is the soft constraint output.

Equation (33) is solved in each control cycle, and a series of control input increments and relaxation factors in the control horizon can be obtained.

$$\Delta U_{dyn,t}^* = \left[\Delta u_{dyn,t}^*, \Delta u_{dyn,t+1}^*, \cdots, \Delta u_{dyn,t+N_C-1}^*\right]^T \tag{34}$$

According to the principle of model predictive control, the first element in the obtained control sequence is acted on the system as the actual control input increment, that is:

$$u_{dyn}(t) = u_{dyn}(t-1) + \Delta u_{dyn,t}^* \tag{35}$$

After entering the next control cycle, repeat the above process, so circular rolling optimization, and ultimately achieve the desired trajectory tracking control.

D. ADDITIONAL YAW MOMENT DISTRIBUTION

Since the tracking trajectory control of the man-machine cooperative driving vehicles considering the driver-in-the-loop is realized by adjusting the additional yaw moment, that is, when the vehicle is running, appropriate braking forces are applied to the corresponding wheels in different states. According to the literature [32]–[34], the existing studies are mostly single-wheel braking and unilateral double-wheel braking strategies. Considering the road adhesion conditions, in order to ensure the braking stability and generate

$$\dot{\xi}_{dyn} = A_{dyn}(t)\,\xi_{dyn}(t) + B_{dyn}(t)\,u_{dyn}(t) \tag{28}$$

$$A_{dyn}(t) = \frac{\partial f_{dyn}}{\partial \xi_{dyn}}$$

$$= \begin{bmatrix} \frac{\partial f_{\dot{x}}}{\partial \dot{x}} & \dot{\varphi} + \frac{2C_{cf}\delta_f}{m\dot{x}} & 0 & \dot{y} + \frac{2aC_{cf}\delta_f}{m\dot{x}} & 0\ 0 \\ \frac{\partial f_{\dot{y}}}{\partial \dot{x}} & -\frac{2\left(C_{cf}+C_{cr}\right)}{m\dot{x}} & 0 & -\dot{x} + \frac{2\left(bC_{cr}-aC_{cf}\right)}{m\dot{x}} & 0\ 0 \\ 0 & 0 & 0 & 1 & 0\ 0 \\ \frac{\partial f_{\dot{\varphi}}}{\partial \dot{x}} & \frac{2\left(bC_{cr}-aC_{cf}\right)}{I_z\dot{x}} & 0 & -\frac{2\left(a^2C_{cf}+b^2C_{cr}\right)}{I_z\dot{x}} & 0\ 0 \\ \cos\varphi & -\sin\varphi & -\dot{x}\sin\varphi - \dot{y}\cos\varphi & 0 & 0\ 0 \\ \sin\varphi & \cos\varphi & \dot{x}\cos\varphi - \dot{y}\sin\varphi & 0 & 0\ 0 \end{bmatrix} \tag{29}$$

$$B_{dyn}(t) = \frac{\partial f_{dyn}}{\partial u_{dyn}} = \begin{bmatrix} 0\ 0\ 0\ \frac{1}{I_z}\ 0\ 0 \end{bmatrix}^T \tag{30}$$

greater additional yaw moment, this paper adopts a unilateral double-wheel braking strategy. Therefore, after the model predictive controller calculates the additional yaw moment required to track the emergency collision avoidance trajectory, it needs to be properly distributed.

The tire adhesion ellipse is described as:

$$F_{xij}^2 + F_{yij}^2 \leq \mu^2 F_{zij}^2 \tag{36}$$

where F_{zij} is the vertical load of the ijth wheel.

The longitudinal and lateral tire forces can be described as:

$$\begin{aligned} 0 \leq F_{xij} &\leq \sqrt{\mu^2 F_{zij}^2 - F_{yij}^2} \\ 0 \leq F_{yij} &\leq \sqrt{\mu^2 F_{zij}^2 - F_{xij}^2} \end{aligned} \tag{37}$$

Therefore, to make full use of the adhesion condition and ignore the transfer of axle-load during motion, the additional yaw moment generated by unilateral front and rear wheel braking is allocated according to the vertical load ratio.

1) When $\Delta M_z \geq 0$, the additional yaw moment of each wheel is described as:

$$\begin{aligned} \Delta M_{zfl} &= \frac{F_{zfl}}{F_{zfl} + F_{zrl}} \Delta M_z \\ \Delta M_{zrl} &= \frac{F_{zrl}}{F_{zfl} + F_{zrl}} \Delta M_z \\ \Delta M_{zfr} &= 0 \\ \Delta M_{zrr} &= 0 \end{aligned} \tag{38}$$

2) When $\Delta M_z < 0$, the additional yaw moment of each wheel is described as:

$$\begin{aligned} \Delta M_{zfl} &= 0 \\ \Delta M_{zrl} &= 0 \\ \Delta M_{zfr} &= \frac{F_{zfr}}{F_{zfr} + F_{zrr}} \Delta M_z \\ \Delta M_{zrr} &= \frac{F_{zrr}}{F_{zfr} + F_{zrr}} \Delta M_z \end{aligned} \tag{39}$$

VI. CO-SIMULATION AND ANALYSIS

In this section, three groups of simulation cases, including the no control vs. MPC control test, the change parameter simulation test, and the PID vs. MPC control test, are presented to evaluate the effectiveness and superiority of the proposed control method. The first and second groups are used to verify the effectiveness of the man-machine cooperative driving vehicle emergency collision avoidance path planning and trajectory tracking control algorithm, and the third group to verify the superiority. Matlab/Simulink-CarSim are used to establish a co-simulation test platform. The simulation parameters are shown in Table 3, and the model is shown in Fig. 8.

A. ALGORITHM EFFECTIVENESS VERIFICATION

To verify the excellent effectiveness of the control algorithm, two groups of contrast simulation tests are set up.

TABLE 3. Intelligent vehicle related parameters.

Symbol	Parameters	Values
a	Distance from the center of mass to the front-axle	1.183m
b	Distance from the center of mass to the rear-axle	1.420m
D_W	Distance between wheels	1.5m
D_{La}	Front overhang	0.82m
B	Vehicle width	1.706m
m	Total vehicle mass	1305kg
I_z	Moment of inertia about the z-axis	2612kg·m^2

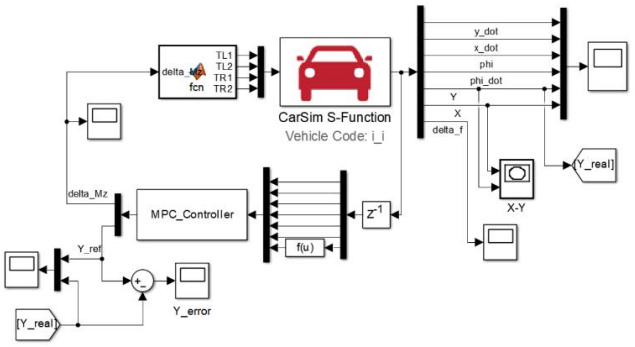

FIGURE 8. Matlab/Simulink-CarSim co-simulation model.

Group I: Contrast simulation test of stress steering collision avoidance about no control and MPC control. The host vehicle was set at a speed of 20m/s on the road with the adhesion coefficient of 0.85, and the lane width was 3.75m. After driving 40 meters, the driver suddenly found that there was a stationary vehicle in the front 20 meters, which was the same as the host vehicle, and the host vehicle was forced to avoid collision by steering. The simulation results of stress steering collision avoidance with no control and MPC control are shown in Fig. 9.

The results in Fig. 9(a) show that, the host vehicle with no control when the stress steering collision avoidance will produce a large lateral displacement, the maximum lateral displacement is 6.178m, which will collide with the road guardrail at 5.625m. However, the planned collision avoidance path can be better tracked during MPC control, therefore avoiding the collision. It can be found from Fig. 9(b-d) that, the host vehicle with no control has a larger yaw rate and lateral acceleration, which can cause the vehicle's stability to deteriorate. Compared with the no control, the MPC control effectively improves the stability of the vehicle during collision avoidance. The yaw rate of the controlled vehicle decreases from 22.75°/s to 13.99°/s, the lateral acceleration decreases from 6.53m/s^2 to 4.77m/s^2, and the sideslip angle of the mass center decreases from 2.17° to 1.93°. It can be seen that the designed control algorithm has excellent effectiveness for stress steering collision avoidance.

Group II: Contrast simulation test of stress steering collision avoidance under different speeds, different road adhesion coefficients, and different driver stress angles.

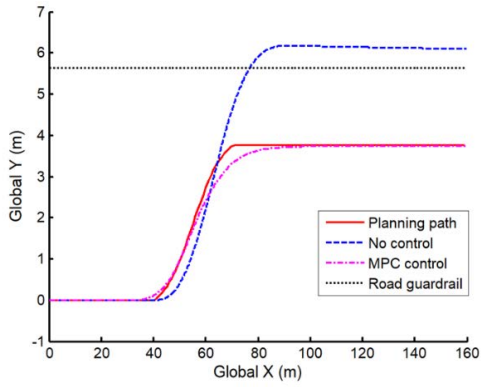

(a) Vehicle collision avoidance path

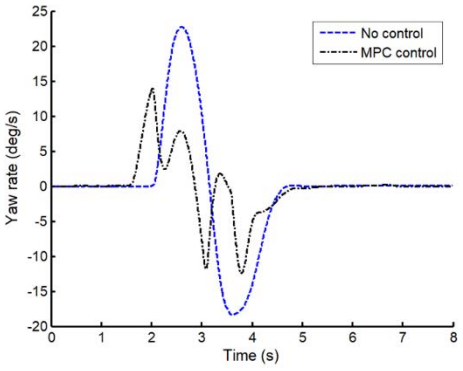

(b) Vehicle yaw rate

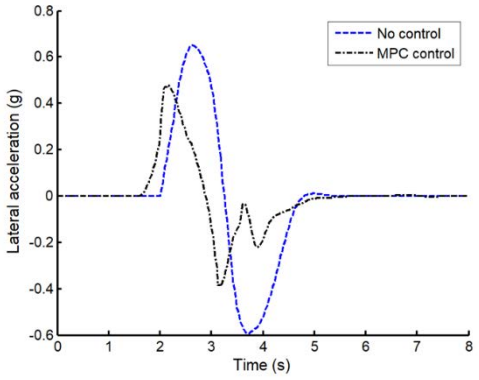

(c) Vehicle lateral acceleration

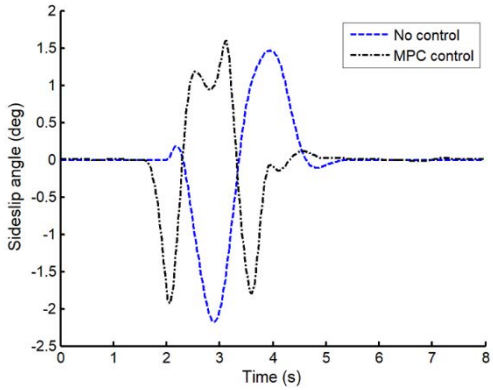

(d) Vehicle sideslip angle

FIGURE 9. Group I.

In condition one, the host vehicle was set to speeds of 20m/s, 25m/s, and 30m/s on the road with the adhesion coefficient of 0.85, and the lane width was 3.75m. After driving 40 meters, the driver suddenly found that there was a stationary vehicle in the front of 20 meters, which was the same as the host vehicle, and the host vehicle was forced to avoid collision by steering. The peak steering angle was 77°. The simulation results are shown in Fig. 10(a-c). In condition two, only the road adhesion coefficient was changed to 0.85, 0.70, and 0.55 respectively, and other conditions remained unchanged. The simulation results are shown in Figure 10(a), (d), and (e). In condition three, only the steering wheel angle peak was changed to 77°, 87°, and 97°, respectively, and other conditions remained unchanged. The simulation results are shown in Fig. 10(a), (f), and (g).

The results in Fig. 10(a-c) show that, with the increase of speed, the effect of additional yaw moment makes the controlled vehicles can follow the designed path better to avoid collision. However, if the speed is too high, the tracking error will be too large at 60m, and the controlled vehicle has the risk of collision with the front stationary vehicle. It can be found from Fig. 10(a), (d), and (e) that, with the decrease of the road adhesion coefficient, the effect of the additional yaw moment makes the controlled vehicle can also track the designed path better to avoid a collision. But if the road adhesion coefficient is too low, which will lead to too large tracking error at the late stage of steering collision avoidance and the controlled vehicle has a short-lived risk of rear-axle sideslip. This is because in the condition of low road adhesion coefficient, the road provides less lateral tire force. It can be found from Fig. 10(a), (f), and (g) that, the different driver stress steering wheel angles have less influence on the control system, and the additional yaw moment makes the controlled vehicle can track the designed path well to avoid a collision. The MPC control algorithm is effective in avoiding collisions under different speeds, different road adhesion coefficients, and different driver stress steering angles.

B. ALGORITHM SUPERIORITY VERIFICATION

To verify the excellent superiority of the control algorithm, the MPC is compared with the classical PID, and the third group of contrast simulation test is set up.

Group III: Contrast simulation test of stress steering collision avoidance about PID control and MPC control. The host vehicle was set at a speed of 20m/s on the road with the adhesion coefficient of 0.85, and the lane width was 3.75m. After driving 40 meters, the driver suddenly found that there was a stationary vehicle in the front 20 meters, which was the same as the host vehicle, and the host vehicle was forced to avoid collision by steering. The simulation results of vehicle steering collision avoidance with PID control and MPC control are shown in Fig. 11.

The results in Fig. 11(a) show that, the PID control and MPC control can both track the planned path to

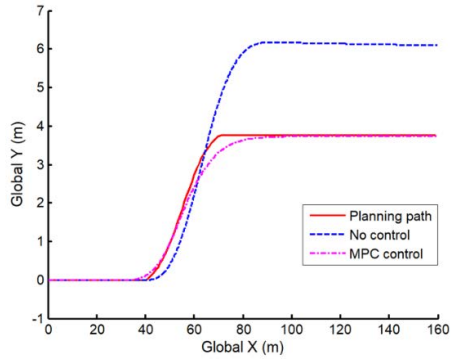

(a) **20m/s, 0.85, 77°**

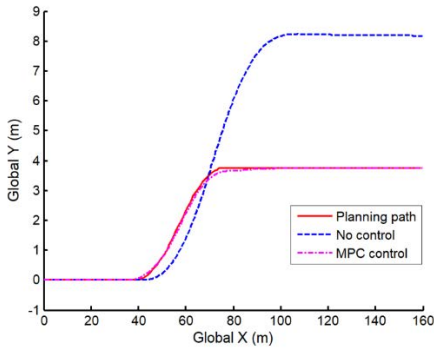

(b) **25m/s, 0.85, 77°**

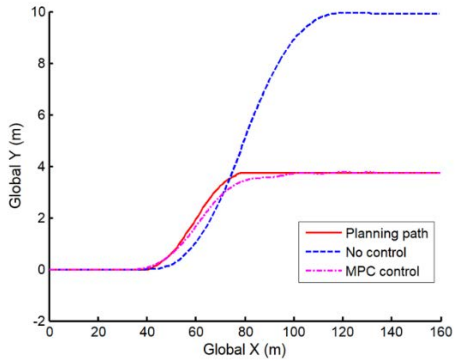

(c) **30m/s, 0.85, 77°**

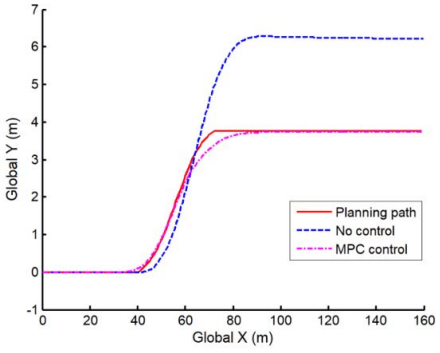

(d) **20m/s, 0.70, 77°**

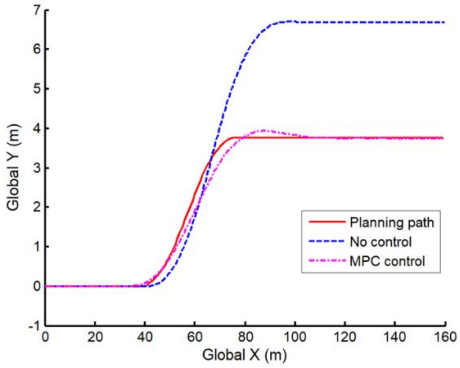

(e) **20m/s, 0.55, 77°**

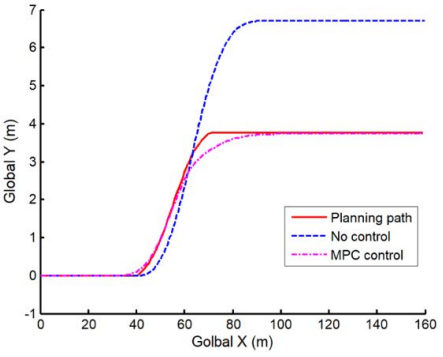

(f) **20m/s, 0.85, 87°**

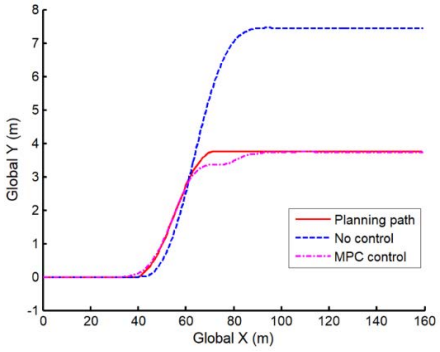

(g) **20m/s, 0.85, 97°**

FIGURE 10. **Group II.**

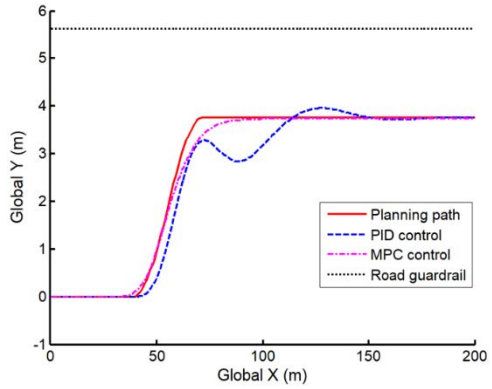

(a) Vehicle collision avoidance path

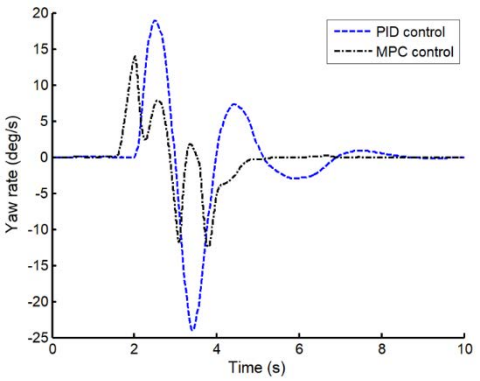

(b) Vehicle yaw rate

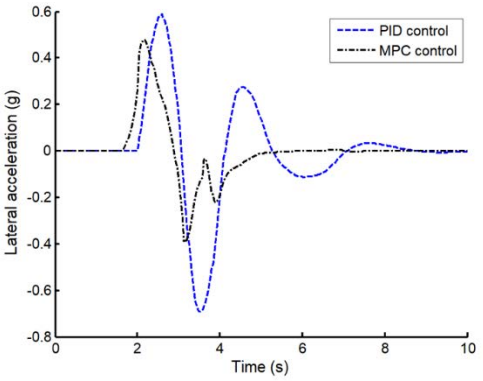

(c) Vehicle lateral acceleration

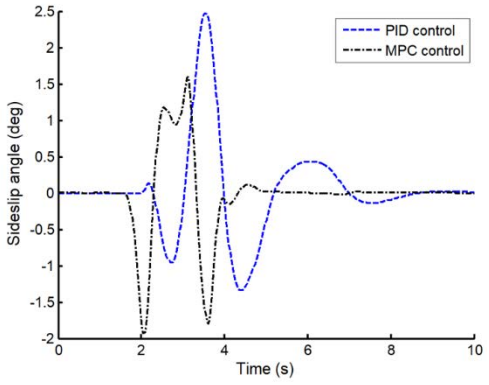

(d) Vehicle sideslip angle

FIGURE 11. Group III.

avoid collision. Compared with the MPC control, the PID control has certain hysteresis and poor tracking effect. This is because MPC is more suitable for the control of nonlinear systems than PID control. Moreover, MPC has a prediction link and can constrain the vehicle intermediate state. It can be found from Fig. 11(b-d) that, the stability of the MPC control is better than that of PID control in vehicle collision avoidance. Compared with the PID control, the MPC control is 25.86% lower in the yaw rate, 19.02% lower in the lateral acceleration, and 21.86% lower in the sideslip angle of the mass center. It can be seen that the designed MPC control algorithm has excellent superiority.

ABBREVIATION

m	Total vehicle mass
a	Distance from the center of mass to the front-axle
b	Distance from the center of mass to the rear-axle
c	Half of the distance between wheels
B	Vehicle width
L	Wheelbase
W	Lane width
μ	Road adhesion coefficient
ε	Relaxation factor
ρ	Weight matrix of relaxation factor
$\dot{x}$	Longitudinal velocity
$\dot{y}$	Lateral velocity
$\ddot{x}$	Longitudinal acceleration
$\ddot{y}$	Lateral acceleration
$\ddot{\varphi}$	Vehicle yaw acceleration
F_{xij}	Longitudinal tire forces of the ijth wheel
F_{yij}	Lateral tire forces of the ijth wheel
F_{zij}	Vertical load of the ijth wheel
F_{lij}	Longitudinal forces of the ijth wheel in the wheel coordinate system
F_{cij}	Lateral forces of the ijth wheel in the wheel coordinate system
I_z	Moment of inertia about the z-axis
δ_f	Front wheel steering angle
d_0	Initial preview distance
$R_{\min}$	Minimum turning radius
ΔM_z	Additional yaw moment
D_{MF}	Longitudinal distance between the vehicle and the obstacle
D_W	Distance between wheels
D_{La}	Front overhang
NDR	Non-driving related
PID	Proportion integral derivative
MPC	Model predictive control
3DOF	Three degrees of freedom
oxy	Vehicle body coordinate system
OXY	Global coordinate system

VII. CONCLUSION

This paper proposed a novel emergency collision avoidance system of man-machine cooperative driving vehicles based on additional yaw moment control. An emergency steering driver model with adaptive preview distance is established. An improved circular arc lane changing path based on the obstacle distance, road adhesion coefficient, vehicle speed, steering wheel stress angle, and driver's linear steering cognition is established. A model predictive control algorithm based on the state change and constraints in the process of vehicle emergency steering is designed. The braking torque of each wheel is adjusted to ensure the accuracy and safety of vehicle tracking by additional yaw moment control. The results of co-simulation show that, the effectiveness and superiority of the designed intelligent vehicle emergency collision avoidance path planning and trajectory tracking control algorithm.

It should be noted that this study does not consider some limiting conditions, such as emergency collision avoidance on icy roads with extremely low road adhesion coefficients. The variation of tire nonlinear characteristics throughout the whole collision avoidance process is also not considered. Meanwhile, this paper does not carry out real vehicle test verification. These will be considered in our future work to expand the future applications of the algorithm.

REFERENCES

[1] Y. Rasekhipour, A. Khajepour, S.-K. Chen, and B. Litkouhi, "A potential field-based model predictive path-planning controller for autonomous road vehicles," *IEEE Trans. Intell. Transp. Syst.*, vol. 18, no. 5, pp. 1255–1267, May 2017.

[2] J. Ji, A. Khajepour, W. W. Melek, and Y. Huang, "Path planning and tracking for vehicle collision avoidance based on model predictive control with multiconstraints," *IEEE Trans. Veh. Technol.*, vol. 66, no. 2, pp. 952–964, Feb. 2017.

[3] J. Cao, C. Song, S. Peng, S. Song, X. Zhang, and F. Xiao, "Trajectory tracking control algorithm for autonomous vehicle considering cornering characteristics," *IEEE Access*, vol. 8, pp. 59470–59484, 2020.

[4] X. He, Y. Liu, C. Lv, X. Ji, and Y. Liu, "Emergency steering control of autonomous vehicle for collision avoidance and stabilisation," *Vehicle Syst. Dyn.*, vol. 57, no. 8, pp. 1163–1187, Oct. 2018.

[5] H. E. B. Russell, L. K. Harbott, I. Nisky, S. Pan, A. M. Okamura, and J. C. Gerdes, "Motor learning affects car-to-driver handover in automated vehicles," *Sci. Robot.*, vol. 1, Dec. 2016, Art. no. eaah5682.

[6] I. Othersen, I. Petermann-Stock, N. Schoemig, and T. Fuest, "Method development and interaction cognitive driver take-over ability after piloted driving," *ATZelektronik worldwide*, vol. 13, no. 2, pp. 28–33, Apr. 2018.

[7] C. Sentouh, A.-T. Nguyen, M. A. Benloucif, and J.-C. Popieul, "Driver-automation cooperation oriented approach for shared control of lane keeping assist systems," *IEEE Trans. Control Syst. Technol.*, vol. 27, no. 5, pp. 1962–1978, Sep. 2019.

[8] S. Ding, "The research about risk situation assessment and lane-change trajectory tracking control of intelligent vehicles," M.S. thesis, College Mech. Vehicle Eng., Hunan Univ., Hunan, China, 2018.

[9] A. A. Neto, D. G. Macharet, and M. F. M. Campos, "Feasible RRT-based path planning using seventh order Bézier curves," in *Proc. IEEE/RSJ Int. Conf. Intell. Robots Syst.*, Taipei, Taiwan, Oct. 2010, pp. 1445–1450.

[10] A. Norouzi, R. Kazemi, and S. Azadi, "Vehicle lateral control in the presence of uncertainty for lane change maneuver using adaptive sliding mode control with fuzzy boundary layer," *Proc. Inst. Mech. Eng., I, J. Syst. Control Eng.*, vol. 232, no. 1, pp. 12–28, Jan. 2018.

[11] A. Norouzi, M. Masoumi, A. Barari, and S. Farrokhpour Sani, "Lateral control of an autonomous vehicle using integrated backstepping and sliding mode controller," *Proc. Inst. Mech. Eng., K, J. Multi-body Dyn.*, vol. 233, no. 1, pp. 141–151, Mar. 2019.

[12] M. Elsisi, K. Mahmoud, M. Lehtonen, and M. M. F. Darwish, "An improved neural network algorithm to efficiently track various trajectories of robot manipulator arms," *IEEE Access*, vol. 9, pp. 11911–11920, 2021.

[13] X. Zhang and X. Zhu, "Autonomous path tracking control of intelligent electric vehicles based on lane detection and optimal preview method," *Expert Syst. Appl.*, vol. 121, pp. 38–48, May 2019.

[14] Y. Yoon, J. Shin, H. J. Kim, Y. Park, and S. Sastry, "Model-predictive active steering and obstacle avoidance for autonomous ground vehicles," *Control Eng. Pract.*, vol. 17, no. 7, pp. 741–750, Jul. 2009.

[15] T. Shim, G. Adireddy, and H. Yuan, "Autonomous vehicle collision avoidance system using path planning and model-predictive-control-based active front steering and wheel torque control," *Proc. Inst. Mech. Eng., D, J. Automobile Eng.*, vol. 226, no. 6, pp. 767–778, Jun. 2012.

[16] C. Sun, X. Zhang, Q. Zhou, and Y. Tian, "A model predictive controller with switched tracking error for autonomous vehicle path tracking," *IEEE Access*, vol. 7, pp. 53103–53114, 2019.

[17] J. Tian, J. Ding, Y. Tai, and N. Chen, "Hierarchical control of nonlinear active four-wheel-steering vehicles," *Energies*, vol. 11, no. 11, p. 2930, Oct. 2018.

[18] H. Cheng, "Research on driver steering model based on two-point preview," M.S. thesis, College Energy Power Eng., Nanjing Univ., Jiangsu, China, 2016.

[19] J. Xie, X. Xu, F. Wang, and L. Chen, "Modeling adaptive preview time of driver model for intelligent vehicles based on deep learning," *Proc. Inst. Mech. Eng., I, J. Syst. Control Eng.*, vol. 236, no. 2, pp. 355–369, Jun. 2021.

[20] X. Zhou, H. Jiang, A. Li, and S. Ma, "A new single point preview-based human-like driver model on urban curved roads," *IEEE Access*, vol. 8, pp. 107452–107464, 2020.

[21] C. Yuan, S. Weng, J. Shen, L. Chen, Y. He, and T. Wang, "Research on active collision avoidance algorithm for intelligent vehicle based on improved artificial potential field model," *Int. J. Adv. Robotic Syst.*, vol. 17, no. 3, May 2020, Art. no. 172988142091123.

[22] S. Krishna, S. Narayanan, and S. Denis Ashok, "Fuzzy logic based yaw stability control for active front steering of a vehicle," *J. Mech. Sci. Technol.*, vol. 28, no. 12, pp. 5169–5174, Dec. 2014.

[23] W. Chen, X. Liu, H. Huang, and H. Yu, "Research on side slip angle dynamic boundary control for vehicle stability control considering the impact of road surface," *J. Mech. Eng.*, vol. 48, no. 14, pp. 112–118, Jul. 2012.

[24] C. Xia, X. Li, and E. Zheng, "Research on active anti-roll control application in the stability of vehicle," *Mach. Des. Manuf.*, vol. 4, pp. 35–38, Apr. 2015.

[25] J. Guo, "Research on control algorithm and performance evaluation method of vehicle electronic stability program," Ph.D. dissertation, College Automot. Eng., Jilin Univ., Jilin, China, 2011.

[26] P. Falcone, H. E. Tseng, F. Borrelli, J. Asgari, and D. Hrovat, "MPC-based yaw and lateral stabilisation via active front steering and braking," *Veh. Syst. Dyn.*, vol. 46, no. S1, pp. 611–628, Sep. 2008.

[27] C. Yuan and Y. Sun, "Research on lane-changing collision avoidance system of intelligent vehicle based on extension control," *J. Chongqing Univ. Tech.*, vol. 34, no. 9, pp. 29–38, Apr. 2020.

[28] K. Lee and D. Kum, "Collision avoidance/mitigation system: Motion planning of autonomous vehicle via predictive occupancy map," *IEEE Access*, vol. 7, pp. 52846–52857, 2019.

[29] Y. Liang, Y. Li, L. Zheng, Y. Yu, and Y. Ren, "Yaw rate tracking-based path-following control for four-wheel independent driving and four-wheel independent steering autonomous vehicles considering the coordination with dynamics stability," *Proc. Inst. Mech. Eng., D, J. Automobile Eng.*, vol. 235, no. 1, pp. 260–272, Jan. 2021.

[30] M. Ataei, A. Khajepour, and S. Jeon, "Model predictive control for integrated lateral stability, traction/braking control, and rollover prevention of electric vehicles," *Vehicle Syst. Dyn.*, vol. 58, no. 1, pp. 49–73, Jan. 2020.

[31] U. Z. A. Hamid, M. H. M. Ariff, H. Zamzuri, Y. Saito, M. A. Zakaria, M. A. A. Rahman, and P. Raksincharoensak, "Piecewise trajectory replanner for highway collision avoidance systems with safe-distance based threat assessment strategy and nonlinear model predictive control," *J. Intell. Robot. Syst.*, vol. 90, nos. 3–4, pp. 363–385, Jun. 2018.

[32] Q. Cui, R. Ding, X. Wu, and B. Zhou, "A new strategy for rear-end collision avoidance via autonomous steering and differential braking in highway driving," *Vehicle Syst. Dyn.*, vol. 58, no. 6, pp. 955–986, Apr. 2019.

[33] C. Tian, "Research on integrated control strategy of active front steering and direct yaw control based on the Kalman filter," M.S. thesis, College Mech. Vehicle Eng., Hunan Univ., Hunan, China, 2017.
[34] Z. Wei, Q. Wang, H. Wang, W. Chen, and X. Lian, "Predictive control for lane departure prevention with two-stage warning based on coordination of active steering and differential braking," *Automot. Eng.*, vol. 41, no. 8, pp. 934–943, Aug. 2019.

CHAOCHUN YUAN was born in Xuzhou, Jiangsu, China, in 1978. He received the B.E. degree from Jiangsu Polytechnic University, in 2000, and the Ph.D. degree from Jiangsu University, in 2007. He is currently a Professor with the Automotive Engineering Research Institute, Jiangsu University. His research interests include intelligent automotive and vehicle active safety. He is an Online Review Expert of the National Natural Science Foundation of China and the Director of the Jiangsu Automotive Engineering Society.

SONGLIN LV was born in Wuhu, Anhui, China, in 1996. He received the B.E. degree from the Harbin University of Science and Technology, in 2019. He is currently pursuing the master's degree in vehicle engineering with the Automotive Engineering Research Institute, Jiangsu University. His research interests include man-machine cooperative driving vehicle and vehicle dynamic systems.

JIE SHEN is the Editor-in-Chief of *International Journal of Modelling and Simulation*, which is an EI-indexed, peer-reviewed research journal in the field of modeling and simulation. He served as an editorial board member for two international journals, an organizer for eight international conferences, an associate editor of two international conference proceedings, a program committee member for 20 international conferences, a session chair for 13 international or national conferences, a board member for three international or national-level technical committees, and a member for various committees at department and campus levels within the University of Michigan–Dearborn.

LONG CHEN was born in Jingjiang, Jiangsu, China, in 1958. He received the Ph.D. degree from Jiangsu University, in 2006. He is currently a Professor with the Automotive Engineering Research Institute, Jiangsu University. His research interests include electric automobile and transportation planning. He is also the Vice Chairperson of the China Society of Automotive Engineering.

YOUGUO HE was born in Huludao, Liaoning, China, in 1977. He received the B.E. degree from the Liaoning University of Technology, in 2000, and the Ph.D. degree from Northeastern University, in 2008. He is currently an Associate Professor with the Automotive Engineering Research Institute, Jiangsu University. His research interests include vehicle active safety and vehicle control systems.

SHUOFENG WENG was born in Suqian, Jiangsu, China, in 1995. He received the B.E. degree from Jiangsu University, in 2016, where he is currently pursuing the Ph.D. degree with the Automotive Engineering Research Institute. His research interests include path planning of intelligent vehicle and vehicle active safety.